Available online at www.sciencedirect.com
SCIENCE DIRECT®
Journal of Molecular Catalysis A: Chemical 228 (2005) 35–45
JOURNAL OF MOLECULAR CATALYSIS A: CHEMICAL
www.elsevier.com/locate/molcata

Hydrocarbon conversion on palladium catalysts

D. Stacchiola, F. Calaza, T. Zheng, Wilfred T. Tysoe*

Department of Chemistry and Biochemistry, Laboratory for Surface Studies, University of Wisconsin-Milwaukee, Milwaukee, WI 53211, USA

Available online 11 November 2004

Abstract

The reaction pathways for acetylene trimerization and hydrogenation, and ethylene hydrogenation, catalyzed by palladium, are explored using a range of surface-sensitive techniques. Reflection–absorption infrared spectroscopy (RAIRS) and low-energy electron diffraction (LEED) show that ethylene is di-σ-bonded on clean Pd(1 1 1), but forms a π-bonded species on a hydrogen pre-covered surface, where the transformation is induced by sub-surface hydrogen. Catalytic ethylene hydrogenation proceeds on an ethylidyne-covered Pd(1 1 1) surface, and it is found that ethylene can still adsorb onto palladium in spite of the presence of an ethylidyne overlayer, and is still in a di-σ-configuration. The rates of ethylidyne formation, and removal by hydrogen are measured independently, where the latter rate is found to be first order in hydrogen pressure. The ethylidyne coverage is measured under reaction conditions as a function of $P(H_2)/P(C_2H_4)$ and found to decrease to ∼1/3 of saturation. Benzene is formed from acetylene on clean Pd(1 1 1) via a metallocyclic C_4H_4 intermediate. This further reacts with a third acetylene to form benzene. However, catalytic cyclotrimerization proceeds in the presence of a carbonaceous layer, which consists of vinylidene species (CH_2=C=). Thus, at high pressures, benzene is formed by reaction between acetylene adsorbed on the vinylidene-covered palladium surface and adsorbed vinylidene itself. The addition of high pressures of hydrogen to the reaction mixture forms a more open surface covered by a mixture of ethylidyne and vinylidene species, rationalizing the observed increase in the benzene formation rate with the addition of hydrogen.

Keywords: Hydrogenation; Cyclotrimerization; Pd(1 1 1) model catalysts; Reflection–adsorption infrared spectroscopy; Low-energy electron diffraction; Ethylene; Acetylene; Hydrogen; Ethylidyne; Vinylidene

1. Introduction

Palladium-catalyzed acetylene cyclotrimerization and alkene and alkyne hydrogenation provide ideal candidates for fundamental investigations of catalytic reaction pathways. This is because these reactions proceed in ultrahigh vacuum where, for example, benzene is formed in temperature-programmed desorption when a Pd(1 1 1) single crystal is saturated with acetylene [1], and adsorbed atomic hydrogen reacts with acetylene or ethylene to yield ethylene and ethane, respectively [2]. In addition, palladium single crystals catalyze these reactions at high pressures with identical kinetics to those of supported systems.

Palladium-catalyzed hydrogenation of ethylene and acetylene are classical catalytic reactions that have been studied for many years. Early on it was established that adsorbed atomic hydrogen adds across the double or triple bond of the adsorbed hydrocarbon [3–14], in the so-called Horiuti-Polanyi model. These hydrogenation reactions were extensively studied in the classical work of Bond [12] where temperature-dependent hydrogen reaction orders of unity or greater are measured, while the order in alkene or alkyne was found to be negative. The latter effect can be rationalized by assuming that hydrogen adsorption is blocked by the alkene or alkyne, while there is no clear explanation for the hydrogen pressure dependences. It was later discovered that a Pt(1 1 1) single crystal model ethylene hydrogenation catalyst was covered by ethylidyne species during reaction [13], although these react with hydrogen too slowly to account for ethylene formation and were proposed to merely act as spectator species.

More recently, it has been demonstrated that theoretical strategies can be used to calculate catalytic rates [15–18]. This has been achieved by calculating heats of adsorption

* Corresponding author. Tel.: +1 414 2295 222; fax: +1 414 2295 036.
E-mail address: wtt@uwm.edu (W.T. Tysoe).

1381-1169/$ – see front matter © 2004 Elsevier B.V. All rights reserved.
doi:10.1016/j.molcata.2004.09.064

and activation energies quantum mechanically using density functional theory (DFT) and by using these energies as inputs into Monte Carlo calculations to predict reaction rates [19]. Such calculations agree extremely well with measured catalytic rates for acetylene hydrogenation. However, energies calculated by DFT are only accurate to a few kiloJoules per mole, and pre-exponential factors were assumed to be "normal" values, for example, $1 \times 10^{13}\,s^{-1}$ for first-order reactions. Such a good agreement between calculated and measured global rates may therefore arise from a cancellation of errors and does not guarantee that it correctly reproduces all of the elementary reaction steps. Nevertheless, these results do indicate that theory has developed to the point at which realistic connections can be made between theory and experiment.

Acetylene cyclotrimerization was first referred to (to our knowledge) in 1915 [20]. Subsequent studies introduced the proposition that one of the roles of the catalyst was to provide a structural template for benzene synthesis [21], as well as lowering the reaction activation energy. This notion was later borne out experimentally where various tailored surface structures could be fabricated by carefully cutting single crystals to form faces with known orientations [22]. These experiments clearly demonstrated that the hexagonal (1 1 1) face of palladium was far more active for the synthesis of benzene from acetylene than others [23,24].

In the early 1980s, it was shown that a monolayer of acetylene chemisorbed on Pd(1 1 1) reacted to form benzene, a result published almost simultaneously by three groups [1,25–27]. Although the reaction, in this case, is not catalytic, this discovery provided an ideal test system for studying a reasonably complicated organic synthetic reaction pathway in some detail, using a wide array of surface-sensitive strategies. Subsequently, several surfaces were found to catalyze the same reaction [28–31].

The following paper outlines how surface science strategies have resulted in the discovery of various surface species on the (1 1 1) face of palladium and how their roles in the catalytic reaction have been identified. This surface analytical information has been used to paint a picture of the working, catalytically active surface, postulate plausible catalytic reaction pathways, and test them.

2. Experimental methods

A wide range of ultrahigh vacuum experimental strategies was used to attack the problem of understanding the catalytic pathways. These include high-pressure catalytic reactions to monitor reaction kinetics at high-pressures [32] and temperature-programmed desorption (TPD) to monitor similar effects in ultrahigh vacuum [1,27]. Surface species have been scrutinized by X-ray and ultraviolet photoelectron spectroscopies [1]. More recently, laser-induced thermal desorption (LITD) [33–35] and nuclear magnetic resonance spectroscopies [36] have been used to monitor the nature of the surface species. Two techniques deserve particular mention. The first is photoelastic-modulation reflection–absorption infrared spectroscopy (PEM-RAIRS) [37–40], which is used to measure the species present on the surface in the presence of a high pressure (in the Torr range) of reactants, and the second is low-energy electron diffraction (LEED) [41]. As conventionally applied, the analysis of surface structures using LEED requires the presence of an ordered overlayer, which, since many systems, in particular small hydrocarbons on metal surfaces, do not form ordered overlayers, has limited its applicability. Attempts to measure overlayer structures from the diffuse background scattering induced by the presence of a disordered adsorbate have been hampered by the weakness of the diffuse background signal [42]. It has however been demonstrated that the intensities of the (1×1) Bragg spots are modified by the presence of a disordered overlayer by about two orders of magnitude more than the intensity of the diffuse background scattering [43,44]. This therefore can be measured more easily than the background scattering and has proven very effective in measuring structures of disordered overlayer of small hydrocarbons on Pd(1 1 1) surfaces and allowed the results of these structure determinations to be compared with DFT predictions and infrared measurements.

3. Results and discussion

3.1. Ethylene hydrogenation: the structure and chemistry of ethylene on clean and hydrogen-covered Pd(1 1 1)

Measurement of the catalytic ethylene and hydrogen pressure dependences for ethylene hydrogenation yields hydrogen reaction orders slightly larger than unity, and negative reaction orders in ethylene pressure [12]. The structure of ethylene on Pd(1 1 1) has been investigated using RAIRS where adsorbed ethylene yielded vibrational features at ~1103 and 2900 cm^{-1}. Using a correlation diagram constructed using the frequencies of organometallic analogs, it was found that ethylene on clean Pd(1 1 1) was di-σ-bonded [46]. The structure of a disordered overlayer of ethylene was also measured on Pd(1 1 1) from the LEED *I*/*V* curves of the substrate (1×1) Bragg spots [47]. In this case, a global structural search was carried out by calculating the Pendry *R*-factor by allowing one carbon to move over 21 points within a reduced surface Wigner-Seitz cell, and simultaneously varying the azimuthal angle and height. The molecule was constrained to be parallel to the surface with a C–C bond length fixed at 1.45 Å. The best-fit structure was then used as an input into a tensor-LEED program [48] in order to optimize the structure. The resulting structural parameters are displayed in Table 1 and the structure depicted in Fig. 1. This reveals that ethylene is indeed di-σ-bonded on Pd(1 1 1) and adsorbed on a bridge site. It has been found previously using LEED that tilted ethylenic species form on Pt(1 1 1) surfaces [49]

Table 1
Measured distances for di-σ-bonded ethylene on clean Pd(1 1 1) at 80 K from an analysis of the LEED *I*/*E* curves compared with the calculated structure for di-σ-bonded ethylene on Pd(1 1 1)

	80 K	DFT calculation [15,17]
d(C—C) (Å)	1.42 ± 0.03	1.45
d(C_1—Pd) (Å)	1.96 ± 0.04	2.19
d(C_2—Pd) (Å)	1.96 ± 0.04	2.19
d_z(C—Pd) (Å)	1.85 ± 0.03	2.10
Θ_{tilt}(C—C) (°)	2 ± 4	0

so that a tensor-LEED calculation was performed by allowing a tilted species to coadsorb with parallel, di-σ-adsorbed ethylene. The resulting plot of Pendry *R*-factor as a function of the proportion of tilted species is displayed in Fig. 2. This shows a minimum *R*-factor when ∼15% of the overlayer comprises a tilted species, the remaining ∼85% being di-σ-bonded ethylene. The optimum geometry of the tilted species is depicted in Fig. 3 and the structural parameters agree well with the structure of vinyl species calculated from DFT theory [15,19], implying that a small amount of vinyl species is formed during ethylene adsorption on Pd(1 1 1). The properties of vinyl species have been investigated by exposing Pd(1 1 1) to vinyl iodide [50]. The resulting infrared spectra show that the absorbances are sufficiently small that such a low coverage would not be detected by RAIRS. They

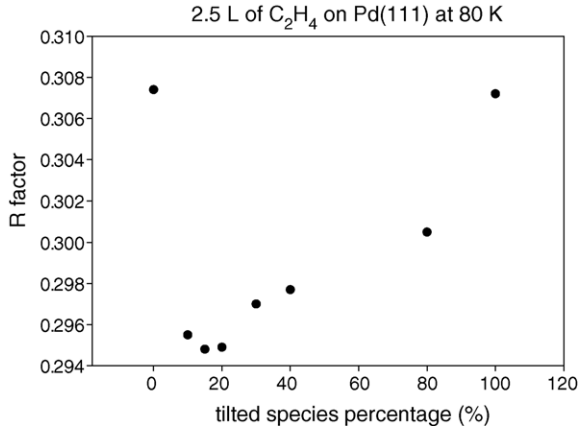

Fig. 2. Plot of Pendry *R*-factor as a function of the percentage of the surface covered by tilted species, where the remainder of the surface is taken to be occupied by di-σ-bonded ethylene.

can react, either by rapid rehydrogenation to ethylene or by forming ethylidyne species [50]. This latter observation suggests a possible route to the formation of ethylidyne species on Pd(1 1 1).

The RAIRS spectra of ethylene on hydrogen-covered Pd(1 1 1) have also been collected and exhibit vibrational frequencies at ∼935 and 3012 cm^{-1}, close to those of gas-phase

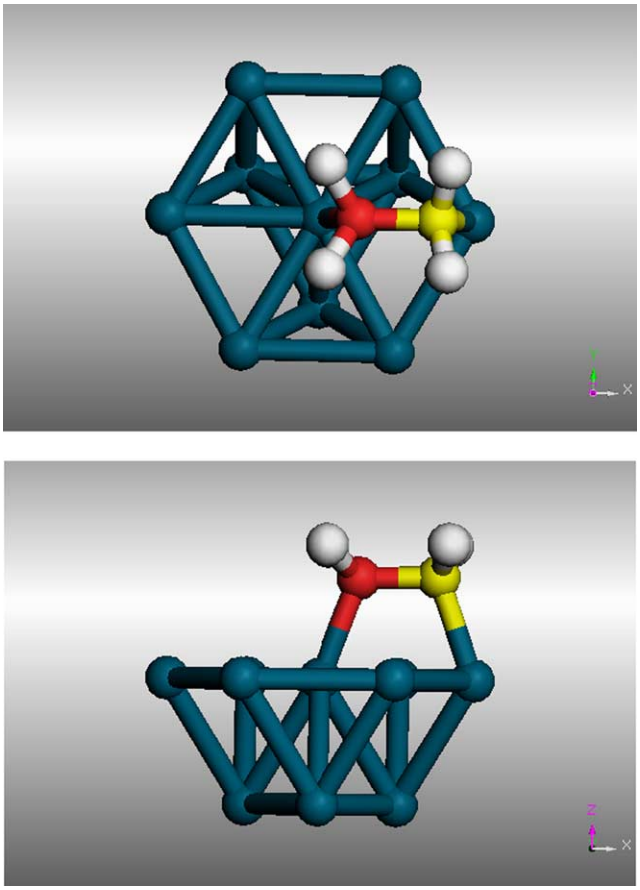

Fig. 1. Schematic depiction of the structure of di-σ-bonded ethylene formed at 80 K on Pd(1 1 1).

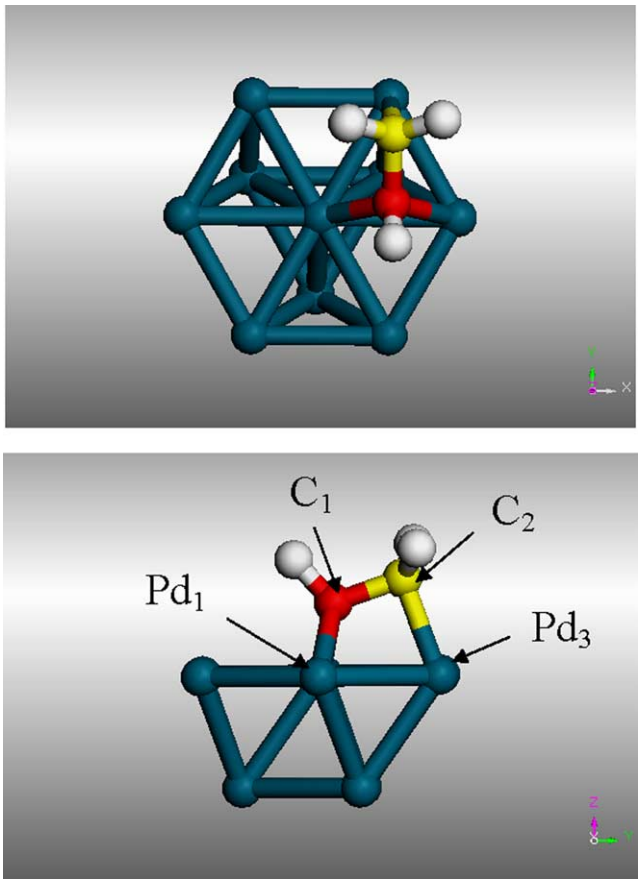

Fig. 3. Schematic depiction of the structure of tilted ethylene formed at low temperature on Pd(1 1 1).

ethylene, implying that ethylene is now π-bonded on the surface [46]. The structure of a disordered overlayer of ethylene on hydrogen-covered Pd(1 1 1) was also determined using LEED [47] where the initial structure was determined using a global search and refined using tensor-LEED. The resulting structural parameters are displayed in Table 2 and compared with the results of DFT calculations [15,19], and the structure is depicted in Fig. 4. This indicates that a change in ethylene adsorption site from bridge to atop is induced by the presence of co-adsorbed hydrogen.

It is well known that hydrogen can either adsorb on or below the surface of metals. It has been proposed that sub-surface hydrogen is the active form for the hydrogenation of alkenes on Ni(1 1 1) [51] and palladium [55,56]. It has also been shown that the proportion of sub-surface and surface hydrogen depends on temperature [52–56] and that, in particular, at a hydrogen coverage of 0.66, at temperatures below 150 K, 60% of the hydrogen is below and 30% on top of the surface, while above 150 K, the hydrogen is equally distributed. This observation can be used to establish whether sub-surface or surface hydrogen is responsible for causing ethylene rehybridization. The experiment is carried out by adsorbing ethylene on hydrogen-covered Pd(1 1 1) at 80 K and measuring the proportion of π- and di-σ-bonded ethylene and comparing these results to a similar experiment carried out at 150 K [57]. Fig. 5 shows the evolution of the infrared spectra of ethylene on hydrogen-covered Pd(1 1 1) at 80 K as a function of hydrogen coverage. This clearly shows the presence of exclusively di-σ-bonded ethylene on clean Pd(1 1 1) and only the π-bonded species on the hydrogen-saturated surface, where the proportion of each varies with hydrogen coverage. The relative coverages of π- and di-σ-bonded ethylene were also measured as a function of hydrogen exposure for adsorption at 150 K. It was found that larger coverages of π-bonded ethylene were detected below 150 K, when sub-surface hydrogen predominates, than at 150 K [57]. Furthermore, the proportions correlated exactly with the relative hydrogen coverages indicating that sub-surface hydrogen causes the ethylene rehybridization, and that surface hydrogen has no effect.

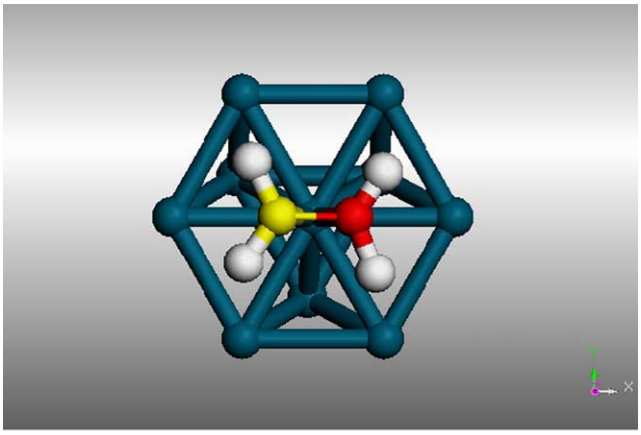

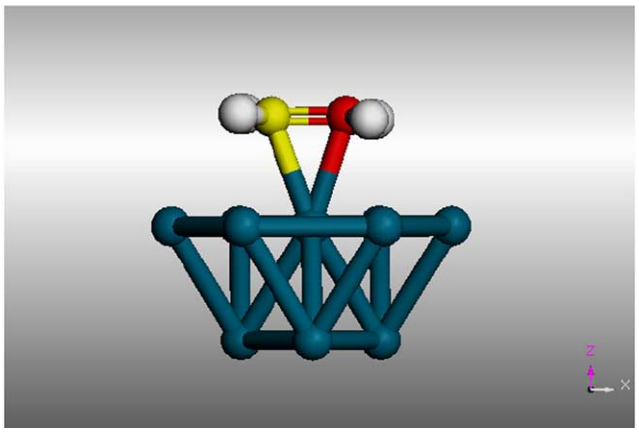

Fig. 4. Depiction of the structure of π-bonded ethylene formed at 80 K on hydrogen-covered Pd(1 1 1).

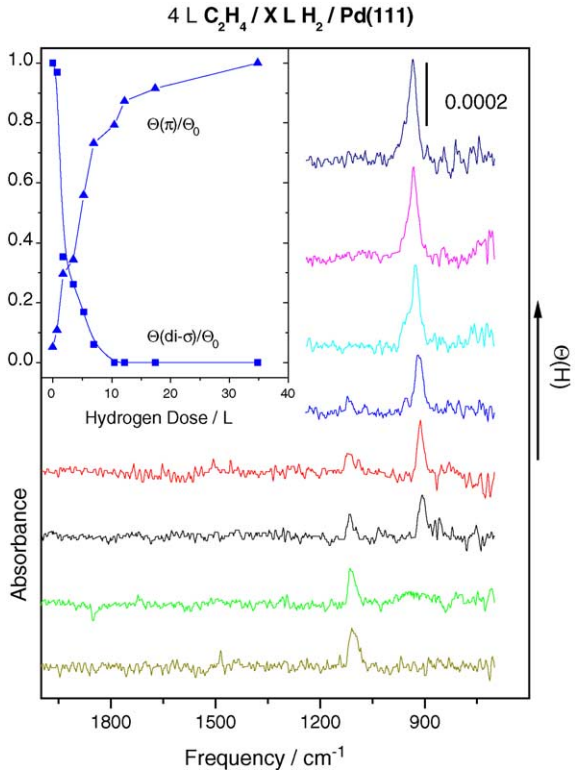

Fig. 5. Plot of the RAIRS spectra of ethylene on hydrogen-covered Pd(1 1 1) showing the evolution from di-σ-bonded ethylene on clean Pd(1 1 1) to π-bonded species on the hydrogen-saturated surface.

Table 2
Calculated distances for π-bonded ethylene on hydrogen-covered Pd(1 1 1) at 80 K from an analysis of the LEED *I*/*E* curves compared with the calculated structure for π-bonded ethylene

	80 K	DFT calculation [17]
d(C—C) (Å)	1.45 ± 0.03	1.40
d(C_1—Pd) (Å)	2.28 ± 0.04	2.24
d(C_2—Pd) (Å)	2.28 ± 0.04	2.24
d_z(C—Pd) (Å)	2.15 ± 0.03	2.13
Θ_{tilt}(C—C) (°)	2 ± 4	0

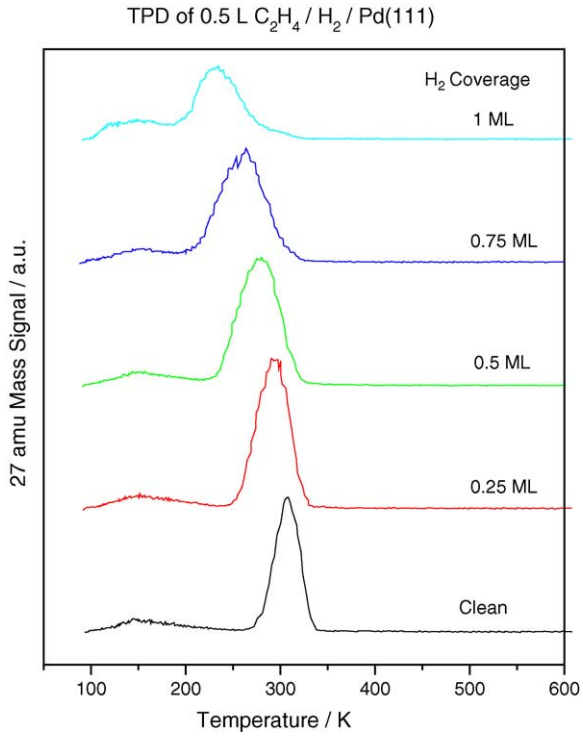

Fig. 6. The TPD spectra of a low coverage of ethylene on hydrogen-covered Pd(1 1 1) displayed as a function of hydrogen coverage.

The TPD spectra of a low coverage of ethylene on hydrogen covered Pd(1 1 1) are displayed in Fig. 6 as a function of hydrogen coverage [58]. This shows that the peak temperature decreases from ~310 K on clean Pd(1 1 1) to ~200 K on the hydrogen-saturated surface. A Redhead analysis of these data [59], using a pre-exponential factor of $1 \times 10^{13}\,s^{-1}$ indicates that this corresponds to a shift in adsorption energy from 79 to 50 kJ/mol on changing from di-σ to π-bonded ethylene. It should be mentioned that the former value for di-σ-bonded ethylene desorption from Pd(1 1 1) is in excellent agreement with spectra simulated from a combination of quantum mechanical and Monte Carlo calculations [18].

Ethane is also formed during TPD and analysis of the results show that π-bonded ethylene, being more weakly bound, hydrogenates more easily than di-σ-bonded ethylene. It has also been demonstrated, by grafting ethyl species onto Pd(1 1 1) by exposing the surface to ethyl iodide that they hydrogenate to ethane more rapidly than ethylene [60]. This indicates that the addition of the first hydrogen to ethylene is the rate-limiting step in the sequential addition of hydrogen atoms to form ethane.

3.2. Roles, formation and removal of ethylidyne species

As in Pt(1 1 1) catalyzed ethylene hydrogenation, a Pd(1 1 1) surface is also covered by ethylidyne species during reaction. It has been shown both by adsorbing CO on ethylidyne-covered Pd(1 1 1) [61] and by LEED measurements that ethylidyne species adsorb on the face-centered cubic (fcc) threefold hollow sites. Once formed, these decompose in TPD to yield hydrogen, where the hydrogen yield can be used to monitor the coverage. This shows that the saturation coverage is 0.25. While it has been suggested that ethylene cannot adsorb onto ethylidyne-saturated Pt(1 1 1) [13], the results of Fig. 7 clearly demonstrate that ethylene chemisorbs on ethylidyne-saturated Pd(1 1 1) [62]. Since the ethylidyne methyl bending mode and the CH_2 bending mode of di-σ-bonded ethylene are almost degenerate, the ethylidyne was formed using d_4-ethylene, which shifts its vibrational modes away from those of ethylene. Clearly evident in Fig. 7 is the mode of d_3-ethylidyne (at 1130 cm^{-1}), easily distinguishable from the feature due to ethylene (at 1100 cm^{-1}), indicating that ethylene does adsorb on ethylidyne-saturated Pd(1 1 1) to form a di-σ-bonded species. Similar experiments in the presence of hydrogen show that π-bonded species are formed [62], so that the surface chemistry is not affected by the presence of ethylidyne except to slightly lower the saturation coverages.

The rate of ethylidyne formation from ethylene can be measured by monitoring the ethylidyne coverage from the hydrogen yield in TPD. The resulting ethylidyne coverages are displayed in Fig. 8 as a function of ethylene exposure at various sample temperatures. In all cases, the coverage saturates at 0.25 monolayers, but the formation rate is temperature dependent. Note also that the rate of ethylidyne formation is rather slow requiring an exposure of ~30 L to saturate the overlayer at 300 K. The data can be analyzed

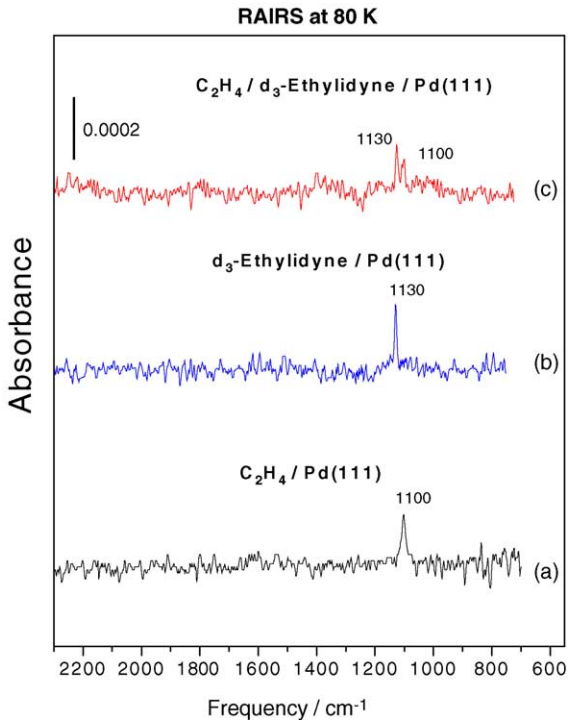

Fig. 7. Infrared spectra of (a) di-σ-bonded ethylene, (b) d_3-ethylidyne, and (c) ethylene adsorbed on d_3-ethylidyne-covered Pd(1 1 1).

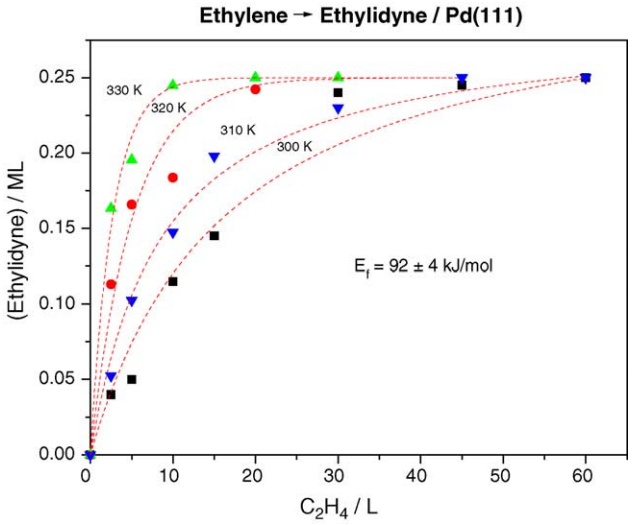

Fig. 8. Plot of ethylidyne coverage as a function of ethylene exposure on clean Pd(1 1 1).

to yield an activation energy to ethylidyne formation of 92 ± 4 kJ/mol. Taking the rate of ethylidyne formation to be equal to $k_1 P(C_2H_4)(0.25 - \Theta(\text{ethylidyne}))$ gives a value of $k_1 \sim 7.1 \times 10^4\ \text{Torr}^{-1}\,\text{s}^{-1}$ at 300 K.

Ethylidyne can only be removed by reaction with hydrogen at high pressures. The ethylidyne removal rate is measured, both on clean Pd(1 1 1) as well as on alumina supported palladium, by monitoring the ethylidyne coverage using infrared spectroscopy in the presence of hydrogen [63]. The resulting *initial* rate of ethylidyne titration from the surface is plotted as a function of hydrogen pressure in Fig. 9. This shows that the rates of ethylidyne titration from both the single crystal and supported catalysts are identical in accord with the observation that a single crystal faithfully mimics the chemistry of the supported system. The data also show that the initial removal rate is first order in hydrogen pressure. This presumably implies an initial pre-equilibrium step between adsorbed ethylidyne and ethylidene. Since it is not possible to measure whether the reaction between ethylidyne and hydrogen yields ethylene or ethane, the subsequent removal steps are not clear. Addition of a second hydrogen would yield an ethyl species, which could undergo β-hydride elimination to form ethylene or rapidly hydrogenate forming ethane. Assuming that the initial rate of ethylidyne removal is given by $k_2 P(H_2)\Theta(\text{ethylidyne})$ yields a value of $k_2 = 3.1 \pm 0.3 \times 10^{-2}\ \text{Torr}^{-1}\,\text{s}^{-1}$ at 300 K.

The ethylidyne coverage is measured using PEM-RAIRS under reaction conditions as a function of $P(H_2)/P(C_2H_4)$, the ratio of the hydrogen to ethylene pressure. Since these react to form ethane, this experiment was carried out by flowing the mixture through the infrared cell at a rate at which no significant ethane was detected in the gas phase by infrared spectroscopy. Again, the ethylidyne coverage was monitored from the intensity of the intense 1329 cm^{-1} methyl-bending mode and the resulting relative ethylidyne coverage is shown in Fig. 10 plotted versus $P(H_2)/P(C_2H_4)$, where the saturation ethylidyne coverage is 0.25. This shows that the ethylidyne coverage decreases as the ethylene to hydrogen ratio increases to ~2, but subsequently remains constant at $\Theta_{\text{rel}} \sim 0.33$ ($\Theta_{\text{abs}} \sim 1/12$ ML).

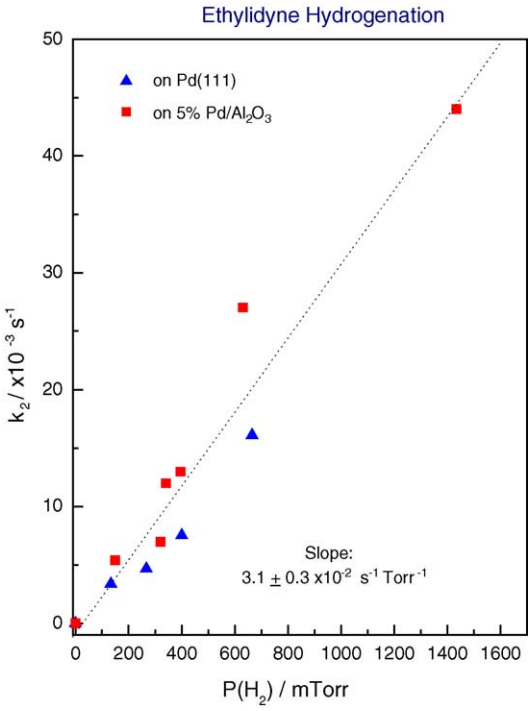

Fig. 9. The initial rate of ethylidyne removal by hydrogen plotted vs. hydrogen pressure, where the ethylidyne coverage was measured under reaction conditions using RAIRS.

Since the rates of ethylidyne removal and formation have been measured independently, assuming that these rates are identical under reaction conditions, and that the system is at steady state yields a relative ethylidyne coverage under

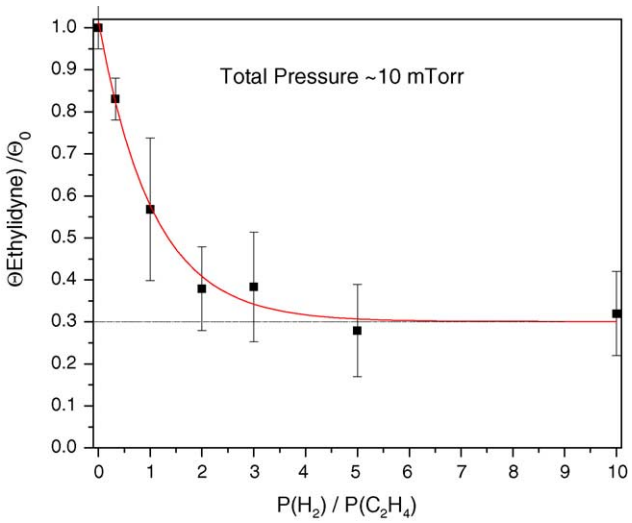

Fig. 10. Plot of the relative ethylidyne coverage under reaction conditions in the presence of a mixture of ethylene and hydrogen, plotted as a function of $P(H_2)/P(C_2H_4)$.

reaction conditions given by Θ(ethylidyne) = (k/r)/(1 + (k/r)), where r is the ratio $P(H_2)/P(C_2H_4)$ and $k = k_1/k_2$. Using the values of k_1 and k_2 measured above indicates that the ethylidyne coverage should be constant over the range of $P(H_2)/P(C_2H_4)$ used experimentally. The shape of the experimentally measured variation *does* fit the formula given above but with a value of $k \sim 2$, several order of magnitude lower than found from the rates of ethylidyne formation and removal. This implies that these rate constants are substantially affected by the presence of other reactants. Hydrogen adsorption is blocked by ethylene [60], which would potentially lower the rate of ethylidyne removal, but this effect would make k even larger. It appears therefore that the rate of ethylidyne formation is substantially decreased by the presence of hydrogen in the reaction mixture. The results described above suggest two possible origins for this effect. First, the presence of sub-surface hydrogen results in the formation of π- rather than di-σ-bonded ethylene [57]. The C–H bond is slightly stronger in ethylene (434 kJ/mol) than ethane (410 kJ/mol) [64] so that dehydrogenation to form vinyl species, proposed to be the precursor to ethylidyne, is less favored. Second, saturation of the surface by hydrogen will limit the surface sites available to accept hydrogen and lower the extent of vinyl formation. It is likely that both effects contribute to the lowering of the ethylidyne formation rate.

The presence of ethylidyne on the surface only slightly affects the saturation ethylene coverage so that on clean Pd(1 1 1) it is ∼0.33, while that on the ethylidyne-saturated surface it is ∼0.25. This implies that removal of a portion of the ethylidyne species under reaction conditions will only have a marginal effect on the reaction kinetics. However, understanding the chemistry of ethylidyne, since it is relatively easily detectable under reaction conditions by PEM-RAIRS, will be beneficial in relating the elementary reaction steps to reactions occurring under realistic conditions.

The reaction pathways identified during ethylene hydrogenation on Pd(1 1 1) are summarized in Scheme 1.

3.3. Acetylene cyclotrimerization

The conversion of acetylene to benzene is catalyzed both by alumina-supported palladium [65] and Pd(1 1 1) single crystals [32].

Following adsorption of acetylene on Pd(1 1 1) at ∼100 K, benzene desorbs in two peaks with a low-temperature state at ∼260 K and a high-temperature state at ∼520 K. Both of these desorption states can be reproduced by adsorbing benzene on the Pd(1 1 1) surface [66] so that product formation is the rate-limiting step in the formation of benzene in TPD. This implies that benzene was synthesized at lower temperatures (below ∼200 K). Direct spectroscopic evidence also points to low-temperature formation of benzene from acetylene [25]. The maximum benzene yield in TPD when the surface is saturated with acetylene, corresponds to the conversion of ∼30% of the adsorbed acetylene with a sample-heating rate of ∼10 K/s. When the heating rate is substantially lowered and the acetylene conversion monitored using laser-induced thermal desorption (LITD), conversions can approach 100% [33–35]. This suggests a branching reaction where the branching ratio is modified by changing the heating rate.

Adsorbed acetylene distorts on Pd(1 1 1) below 200 K so that the carbon atoms are sp^2 hybridized [67–69]. The structure of acetylene has been measured on Pd(1 1 1) by LEED and is shown in Fig. 11 [43]. It has also been demonstrated, by adsorbing dichlorocyclobutene that benzene forms by reaction between acetylene and an intermediate having a stoichiometry C_4H_4 [70,71]. Near-edge X-ray Adsorption Fine Structure (NEXAFS) results, in conjunction with theoretical analyses of these data, allow this species to be identified as a metallacycle [72]. The “template” effect of the hexagonal (1 1 1) face correctly orients the adsorbed C_2H_2 and C_4H_4 species to form benzene [21]. These ideas suggest that the synthesis of benzene in ultrahigh vacuum requires the participation of ∼7 exposed palladium atoms on the surface. A similar model successfully rationalizes the effect of site blocking by oxygen [73] and of Au/Pd alloys [74,75] on the benzene yield. Further confirmation of the participation of C_4 species in the reaction comes from the detection of

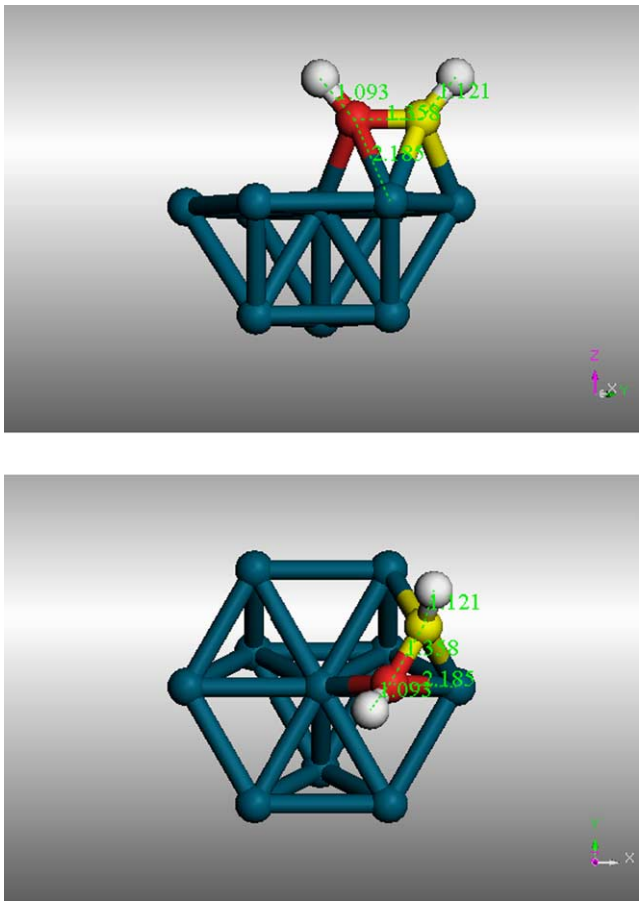

Fig. 11. Structure of acetylene on Pd(1 1 1) measured using LEED.

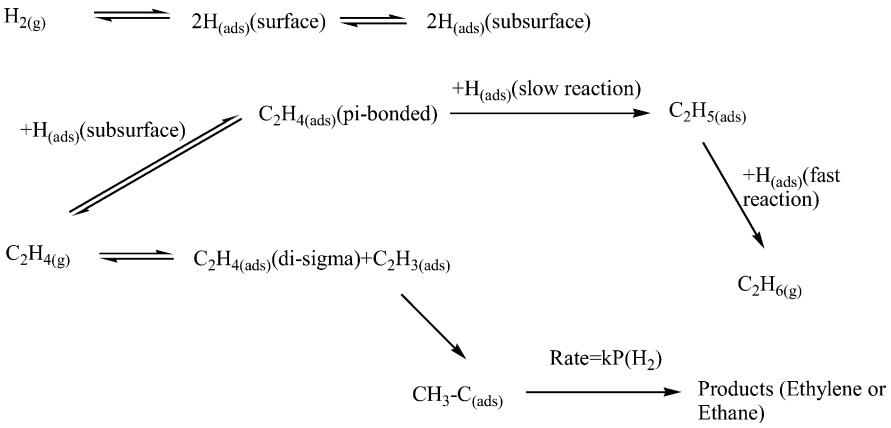

Scheme 1.

heterocyclic products, furan and thiophene, when acetylene is co-adsorbed with oxygen and sulfur, respectively [73,76].

On heating, adsorbed acetylene converts to another species, identified as vinylidene [1,77] with a saturation coverage $\Theta_{max} = 1$ [1]. This is unreactive in ultrahigh vacuum so that heating a vinylidene-covered surface merely desorbs hydrogen at ~450 K and no benzene is formed [1]. In addition, co-adsorption of acetylene and hydrogen on Pd(1 1 1) at ~100 K desorbs ethylene so that the flat lying, rehybridized acetylenic species is the precursor to acetylene hydrogenation, whereas co-adsorbing hydrogen and vinylidene yields no hydrogenation products in TPD [2]. This suggests that the accumulation of unreactive vinylidene species might be responsible for the decrease in cyclotrimerization activity as a function of time found for supported palladium catalysts [65].

These results indicate that benzene is rapidly synthesized from acetylene on clean Pd(1 1 1) via a reaction between a C_4 and C_2 species. During catalysis, however, reaction apparently proceeds in the presence of a carbonaceous layer, which consists of vinylidenes. Unlike ethylidyne, which does not inhibit ethylene adsorption, vinylidene completely prevents subsequent adsorption onto the palladium surface in ultrahigh vacuum (where gas pressures up to $\sim 1 \times 10^{-6}$ Torr can be attained). It has, however, been demonstrated using infrared spectroscopy and molecular beam methods that CO can adsorb onto Pd(1 1 1) in the presence of a saturated vinylidene overlayer when the gas pressure is sufficiently high [78]. This suggests that acetylene might also adsorb onto a vinylidene-covered surface, although it is unlikely that two or three adjacent acetylene molecules can be accommodated as suggested is necessary for benzene synthesis from ultrahigh vacuum data. However, it has been shown that acetylene and vinylidene can react, in homogenous phase, to form a C_4 intermediate in titanium-containing organometallics [79–81]. It is, thus, suggested that acetylene adsorbed on the vinylidene-covered palladium surface can analogously react to form a C_4 species, and eventually benzene as follows:

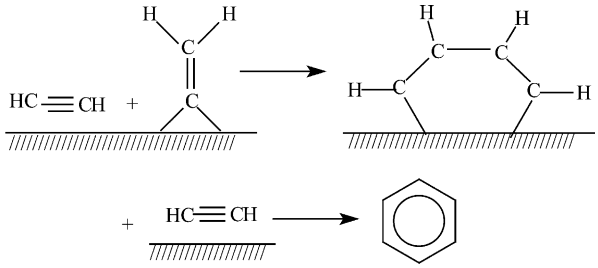

In order to test this hypothesis, a vinylidene-covered surface is prepared using ^{13}C-labelled acetylene [36] where the vinylidene coverage was monitored using nuclear magnetic resonance spectroscopy [82]. These experiments showed that vinylidene is removed by acetylene *at exactly the same rate* at which benzene is formed [36]. This indicates that, under reaction conditions, the benzene formation pathway is different from that found in ultrahigh vacuum where, under catalytic conditions, benzene formation is initiated by a reaction between adsorbed acetylene and vinylidene species, rather than between two adsorbed acetylenes.

3.4. Effect of hydrogen on adsorbed vinylidene

The nature of the surface was examined in the presence of a mixture of acetylene and hydrogen using infrared spectroscopy and the results displayed in Fig. 12a [83]. This reveals that ethylidyne species are formed on the surface and show the ethylidyne coverage increases as a function of hydrogen pressure. Since the saturation coverage of ethylidyne ($\Theta_{sat} = 0.25$) is substantially lower than that of vinylidene ($\Theta_{sat} = 1.0$), this is expected to result in a more open surface. Measuring the total amount of CO that can be accommodated onto the surface shows this to be the case and the results are displayed in Fig. 12b.

In order to probe the reactivity of the more open, ethylidyne-covered surface, this was exposed to acetylene and a TPD experiment carried out [83], and the results are displayed in Fig. 13. The benzene desorption spectra for acetylene on clean Pd(1 1 1) display the low-temperature state due

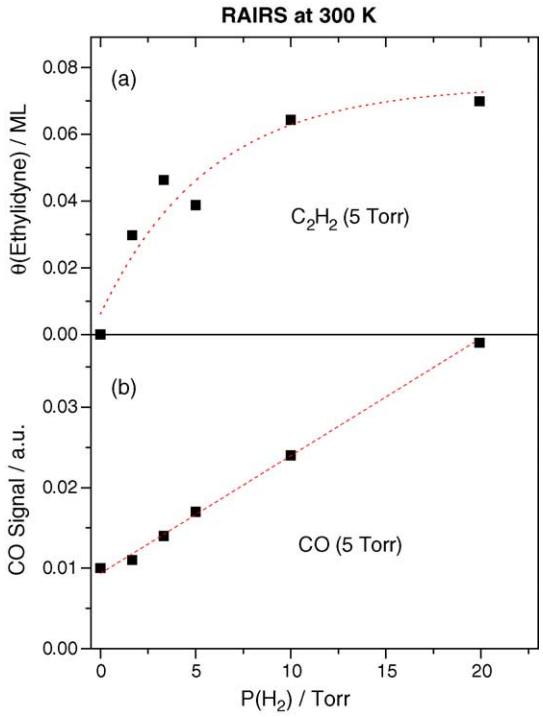

Fig. 12. Plot of (a) the ethylidyne coverage as a function of hydrogen pressure in the presence of 5 Torr of acetylene for reaction at 300 K and (b) the amount of CO adsorbed on the surface following each reaction using a total CO pressure of 5 Torr.

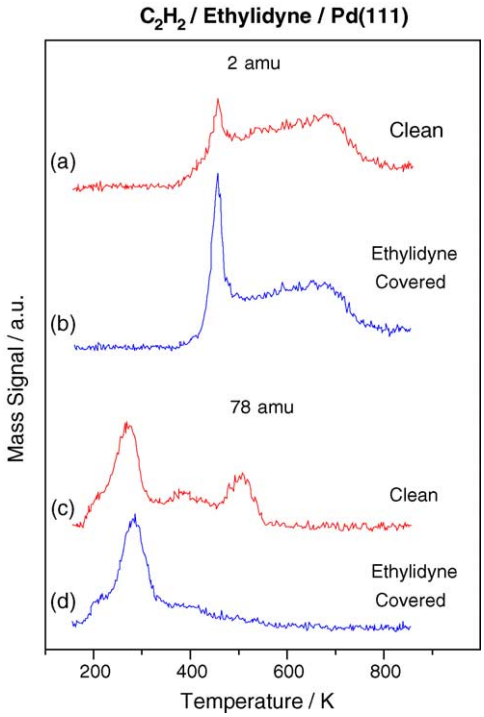

Fig. 13. Hydrogen (2 amu) and benzene (78 amu) temperature-programmed desorption spectra for acetylene adsorbed onto clean and ethylidyne-saturated Pd(1 1 1).

to the desorption of tilted benzene, and the high-temperature state due to the flat-lying species. The low-temperature feature only is found for the ethylidyne-covered surface suggesting that there is insufficient space for the flat-lying species to form on the ethylidyne-covered surface. As noted above, the catalytic rate of benzene formation increases with the addition of hydrogen, and this effect is ascribed to the presence of a more open, partially ethylidyne-covered surface. Ethylene is also formed by the hydrogenation of adsorbed acetylene. The rate of this reaction is also accelerated by the formation of a more open surface as the hydrogen pressure increases, so that hydrogen, in this case, performs two functions; as a reactant and to create more "active sites" on the surface.

3.5. Role of hydrogen in the catalytic hydrogenation of alkenes and alkynes

Hydrogen is evidently a reactant, adding sequentially across the double or triple bonds where the first addition of atomic hydrogen is, in each case, the rate-limiting step in hydrogenation reactions. It, however, performs other functions. It changes the adsorption state of ethylene from more strongly bound di-σ-bonded species that are present on clean Pd(1 1 1), to a more weakly bound, and therefore more reactive, π-bonded species that is formed by the influence of sub-surface hydrogen. It also reacts with strongly bound carbonaceous species, ethylidyne or vinylidene to produce more open surfaces. The importance of each of these latter functions depends on the reaction. In the case of ethylene hydrogenation, ethylene adsorption is only slightly inhibited by the presence of an ethylidyne overlayer so that the decrease in ethylidyne coverage as the hydrogen pressure increases will only slightly accelerate the reaction rate. In this case, however, the presence of sub-surface hydrogen activates adsorbed ethylene such that it hydrogenates more easily. Sub-surface hydrogen has also been suggested to react with adsorbed ethylene to form ethane [51,55,56]. In retrospect, the observations may not be so surprising since extrapolation of surface hydrogen adsorption isotherms measured on Pd(1 1 1) in UHV to the conditions encountered during reaction suggests that the hydrogen overlayer coverage is always close to saturation and varies only very slightly with hydrogen pressure. In spite of this, strong variations are found in hydrogenation rates as a function of hydrogen pressure and the ethylidyne removal rate shows a first-order hydrogen pressure dependence (Fig. 9). Such observations are difficult to rationalize if surface hydrogen is the reactant for these processes.

In the case of acetylene hydrogenation, the conversion of vinylidene into ethylidyne species creates a more open surface, allowing more acetylene to adsorb thereby increasing the reaction rate. It is not yet known whether sub-surface hydrogen similarly weakens acetylene bonding. These additional effects of hydrogen provide a basis for understanding the observed hydrogen reactions orders for both ethylene and acetylene hydrogenation where, in spite of the similar

hydrogen reaction orders in each case, the origin of this effect appears to be different in each case.

4. Conclusions

The surface processes occurring during ethylene and acetylene hydrogenation and acetylene cyclotrimerization have been investigated both in ultrahigh vacuum and at high pressures and a rather complete picture of the participating surface reactions has been obtained. Surface structures measured using low-energy electron diffraction are in excellent agreement with those found using quantum calculations. The ultimate goal in fully understanding catalytic reactions will be to compare the results of DFT and Monte Carlo calculations with the kinetics of elementary reaction steps measured either in ultrahigh vacuum (using TPD) or at high pressures where the nature of the surface is monitored in situ.

Acknowledgments

We gratefully acknowledge support of this work by the U.S. Department of Energy, Division of Chemical Sciences, Office of Basic Energy Sciences, under grant number DE-FG02-92ER14289.

References

[1] W.T. Tysoe, G.L. Nyberg, R.M. Lambert, Surf. Sci. 135 (1983) 128.
[2] R.M. Ormerod, R.M. Lambert, D.W. Bennett, W.T. Tysoe, Surf. Sci. 330 (1995) 1.
[3] G.C. Bond, P.B. Wells, J. Catal. 5 (1965) 65.
[4] G.C. Bond, P.B. Wells, J. Catal. 4 (1965) 211.
[5] T. Yasunobi, I. Yasumori, J. Phys. Chem. 75 (1971) 880.
[6] J.M. Moses, A.H. Weiss, K. Matusek, L. Guczi, J. Catal. 86 (1984) 417.
[7] L.Z. Gua, K.E. Kho, Kinetika I Kataliz. 29 (1988) 381.
[8] R.B. Moyes, D.W. Walker, P.B. Wells, D.A. Whan, E.A. Irvine, Appl. Catal. 55 (1989) 5.
[9] H.R. Adúriz, P. Bodnariuk, M. Dennehy, A. Grgola, Appl. Catal. 58 (1990) 227.
[10] G.C. Bond, P.B. Wells, J. Catal. 5 (1965) 65.
[11] A.N.R. Bos, K. Westerterp, Chem. Eng. Process. 32 (1978) 1.
[12] G.C. Bond, Catalysis by Metals, Academic Press, New York, 1962.
[13] O. Beeck, Discuss Faraday Soc. 8 (1950) 118.
[14] G.C. Bond, P.B. Wells, Adv. Catal. 15 (1964) 91.
[15] M. Neurock, R.A. Van Santen, J. Phys. Chem. B. 105 (2000) 11127.
[16] P.A. Sheth, M. Neurock, C.M. Smith, J. Phys. Chem. B 107 (2003) 2009.
[17] Q. Ge, M. Neurock, Chem. Phys. Lett. 358 (2002) 377.
[18] E.W. Hansen, M. Neurock, Chem. Eng. Sci. 54 (1999) 3411.
[19] V. Pallassana, M. Neurock, V.S. Lusuard, J.J. Lerov, D.D. Kiagten, R.A. Van Santen, J. Phys. Chem. B 106 (2002) 1656.
[20] I. Oppenheim, J.J. Carberry, H.H. Heinemann, G.W. Keulks, J. Turkevich, Soviet Heterogeneous Catalytic Research, Technical Assessment Report, FASEC-TAR-3040, 1985.
[21] Y. Inoue, I. Kojima, S. Moriki, I. Yasumori, Proc. Int. Cong. Catal. Letchworth, UK (1976).
[22] G.A. Somorjai, Chemistry in Two Dimensions: Surfaces, Cornell University Press, Ithaca, 1981.
[23] B. Marchon, Surf. Sci. 162 (1985) 384.
[24] J. Yoshinobu, T. Sekitani, M. Onchi, M. Nishijima, J. Phys. Chem. 94 (1990) 4269.
[25] W. Sesselman, B. Woratschek, G. Ertl, J. Küppers, H. Haberland, Surf. Sci. 130 (1983) 245.
[26] T.M. Gentle, E.L. Muetterties, J. Phys. Chem. 87 (1983) 245.
[27] W.T. Tysoe, G.L. Nyberg, R.M. Lambert, J. Chem. Soc., Chem. Commun. 11 (1983) 623.
[28] N.A. Avery, J. Am. Chem. Soc. 107 (1985) 6711.
[29] C. Xu, J.W. Peck, B.E. Koel, J. Am. Chem. Soc. 115 (1993) 751.
[30] C.J. Badderley, R.M. Ormerod, A.W. Stephenson, R.M. Lambert, J. Phys. Chem. 99 (1995) 5146.
[31] K.G. Pierce, M.A. Barteau, J. Phys. Chem. 115 (1993) 751.
[32] T.G. Rucker, M.A. Logan, E.M. Muetterties, G.A. Somorjai, J. Phys. Chem. 90 (1986) 2703.
[33] I.M. Abdelrehim, T.E. Caldwell, D.P. Land, J. Phys. Chem. 100 (1996) 10265.
[34] I.M. Abdelrehim, N.A. Thornburg, J.T. Sloan, T.E. Caldwell, D.P. Land, J. Am. Chem. Soc. 117 (1995) 9509.
[35] I.M. Abdelrehim, N.A. Thornburg, J.T. Sloan, D.P. Land, Surf. Sci. 298 (1993) L169.
[36] M. Kaltchev, D. Stacchiola, H. Molero, G. Wu, A. Blumenfeld, W.T. Tysoe, Catal. Lett. 60 (1999) 11.
[37] M. Kaltchev, A.W. Thompson, W.T. Tysoe, Surf. Sci. 391 (1997) 145.
[38] T.P. Beebe Jr., J.T. Yates Jr., J. Am. Chem. Soc. 108 (1986) 663.
[39] T.P. Beebe Jr., M.R. Albert, J.T. Yates Jr., J. Catal. 96 (1986) 1.
[40] D. Stacchiola, A.W. Thompson, M. Kaltchev, W.T. Tysoe, J. Vac. Sci. Technol. A20 (2002) 2101.
[41] M.A. Van Hove, S.Y. Tong, Surface Crystallography by LEED, Springer, Berlin, 1979.
[42] J.B. Pendry, D.K. Saldin, Surf. Sci. 145 (1984) 33.
[43] T. Zheng, W.T. Tysoe, H.C. Poon, D.K. Saldin, Surf. Sci. 543 (2003) 19.
[44] H.C. Poon, M. Weinert, D.K. Saldin, D. Stacchiola, T. Zheng, W.T. Tysoe, Phys. Rev. B 69 (2004) 035401.
[46] D. Stacchiola, L. Burkholder, W.T. Tysoe, Surf. Sci. 511 (2002) 215.
[47] T. Zheng, D. Stacchiola, H.C. Poon, D.K. Saldin, W.T. Tysoe, Surf. Sci. 564 (2004) 71.
[48] A. Barbieri, M.A. Van Hove, Symmetrized Automated Tensor LEED package available from M.A. Van Hove.
[49] R. Döll, C.A. Gerken, M.A. Van Hove, G.A. Somorjai, Surf. Sci. 374 (1997) 151.
[50] S. Azad, M. Kaltchev, G. Wu, D. Stacchiola, W.T. Tysoe, J. Phys. Chem. B 104 (2000) 3107.
[51] K.L. Haug, T. Bürgui, T.R. Trautman, S.T. Ceyer, J. Am. Chem. Soc. 120 (1998) 8885.
[52] Sh. Shaikhutdinov, M. Heemeier, B. Baümer, T. Lear, D. Lennon, R.J. Oldman, S.D. Jackson, H.J. Freund, J. Catal. 200 (2001) 330.
[53] Sh. Shaikhutdinov, M. Frank, M. Baümer, S.D. Jackson, R.J. Oldman, J.C. Hemminger, H.J. Freund, Catal. Lett. 80 (2002) 115.
[54] A.M. Doyle, Sh. Shaikhutdinov, S.D. Jackson, H.J. Freund, Agnew. Chem. 42 (2003) 5240.
[55] M.S. Daw, S.M. Foiles, Phys. Rev. B 35 (1987) 2128.
[56] T.E. Felter, E.C. Sowa, M.A. Van Hove, Phys. Rev. B 40 (1989) 891.
[57] D. Stacchiola, W.T. Tysoe, Surf. Sci. 540 (2003) 600.
[58] L. Burkholder, D. Stacchiola, W.T. Tysoe, Surf. Rev. Lett. 10 (2003) 909.
[59] P.A. Redhead, Vacuum 12 (1962) 203.
[60] D. Stacchiola, S. Azad, L. Burkholder, W.T. Tysoe, J. Phys. Chem. B 105 (2001) 11233.
[61] D. Stacchiola, M. Kaltchev, G. Wu, W.T. Tysoe, Surf. Sci. 470 (2000) L32.
[62] D. Stacchiola, W.T. Tysoe, Surf. Sci. 513 (2002) L431.

[63] D. Stacchiola, H. Molero, W.T. Tysoe, Catal. Today 65 (2001) 3.
[64] CRC Handbook of Physics and Chemistry, CRC Press, Boca Raton, FL, 1988.
[65] R.M. Ormerod, R.M. Lambert, J. Chem. Soc., Chem. Commun. 20 (1990) 1421.
[66] A. Ramirez-Cuesta, D. Valladares, A. Velasco, G. Zgrablich, W.T. Tysoe, R.M. Ormerod, R.M. Lambert, J. Phys., C: Condens. Matter 5 (1993) 137.
[67] H. Hoffmann, F. Zaera, R.M. Ormerod, R.M. Lambert, J.M. Yao, L.P. Wang, D.W. Bennett, W.T. Tysoe, Surf. Sci. 268 (1992) 1.
[68] H. Sellars, J. Phys. Chem. 94 (1990) 8329.
[69] G. Pacchioni, R.M. Lambert, Surf. Sci. 304 (1994) 208.
[70] C.H. Patterson, R.M. Lambert, J. Phys. Chem. 92 (1988) 1266.
[71] R.M. Ormerod, C.J. Badderly, R.M. Lambert, Surf. Sci. 259 (1991) L709.
[72] R.M. Ormerod, R.M. Lambert, H. Hoffmann, F. Zaera, J.M. Yao, D.K. Saldin, L.P. Wang, D.W. Bennett, W.T. Tysoe, Surf. Sci. 295 (1993) 277.
[73] R.M. Ormerod, R.M. Lambert, Catal. Lett. 6 (1990) 6871.
[74] C.J. Baddeley, M. Tikhov, C. Hardacre, J.R. Lomas, R.M. Lambert, J. Phys. Chem. 100 (1996) 2189.
[75] C.J. Baddeley, M. Tikhov, R.M. Lambert, Surf. Sci. 314 (1994) 1.
[76] A.J. Gellman, Langmuir 7 (1991) 827.
[77] R.M. Ormerod, R.M. Lambert, H. Hoffmann, F. Zaera, L.P. Wang, D.W. Bennett, W.T. Tysoe, J. Phys. Chem. 92 (1994) 2134.
[78] D. Stacchiola, G. Wu, M. Kaltchev, W.T. Tysoe, J. Chem. Phys. 115 (2001) 3315.
[79] R. Beckhaus, Agnew. Chem. Ed. Engl. 36 (1977) 1686.
[80] R. Beckhaus, J. Oster, B. Gauter, U. Englert, Organometallics 16 (1997) 3902.
[81] R. Beckhaus, J. Sang, T. Wagner, B. Gauter, Organometallics 15 (1996) 1176.
[82] G.C. Levy, R.L. Lichter, G.L. Nelson, Carbon-13 NMR Spectroscopy, Wiley Interscience, New York, 1980.
[83] D. Stacchiola, G. Wu, H. Molero, W.T. Tysoe, Catal. Lett. 71 (2001) 1.